

High quality factor Er-doped Fabry–Perot microcavities by sol–gel processing

Yigang Li^{1,3}, Luís M Fortes¹, Andrea Chiappini², Maurizio Ferrari² and Rui M Almeida¹

¹ Departamento de Engenharia de Materiais/ICEMS, Instituto Superior Técnico/TULisbon, Av. Rovisco Pais, 1049-001 Lisboa, Portugal

² CNR-IFN, Istituto di Fotonica e Nanotecnologie, CSMFO Lab., Via alla Cascata 56/C, Povo, 38123 Trento, Italy

E-mail: yigang.li@ist.utl.pt and ruí.almeida@ist.utl.pt

Received 17 July 2009

Published 23 September 2009

Online at stacks.iop.org/JPhysD/42/205104

Abstract

An optimized sol–gel process was developed to fabricate 1D photonic bandgap structures. Several erbium-doped Fabry–Perot microcavities were prepared and characterized. The thickest sample contained two Bragg mirrors, each having 12 distributed Bragg reflector periods of alternating silicate glass and titania layers. The total thickness of this sample reached $\sim 12\ \mu\text{m}$. The Er^{3+} photoluminescence spectra at $1.5\ \mu\text{m}$ were measured for the microcavities. A quality factor of 250 and an Er^{3+} photoluminescence enhancement of 96 times at $1.5\ \mu\text{m}$ have been reached. The sol–gel processing details, the crystallization of the titania films and the refractive index of the deposited materials are discussed in detail. The simulated optical spectra of the microcavities were found to agree well with the actually measured curves. These results demonstrate that the present sol–gel processing technique is of potential interest for low cost fabrication of 1D photonic bandgap devices.

(Some figures in this article are in colour only in the electronic version)

1. Introduction

Photonic bandgap (PBG) structures, also known as photonic crystals (PCs), are periodic dielectric structures which exhibit a range of frequencies for which electromagnetic wave propagation is forbidden, although the individual component materials are transparent. The original idea was introduced by Yablonovich and John about 20 years ago [1, 2]. A classical example of a one-dimensional (1D) PC is an interference filter (also called a Bragg mirror, BM), which consists of a stack of alternating high and low refractive index dielectric layers and exhibits a frequency region of high reflectivity. The optical thickness of each layer of the BM is $nd = \lambda/4$, where n and d are the refractive index and thickness, respectively, and λ is the wavelength of maximum reflectivity. This forbidden frequency range is also called a ‘stop band’. Moreover, when the BM structure has a defect, such as a missing layer, this will cause the occurrence of an allowed state (‘pass band’) localized inside the stop band at the resonance wavelength, λ . This

particular structure is called a Fabry–Perot (F–P) microcavity [3–9]. The F–P microcavity increases the functionality of the 1D PBG structures [10]; for instance, it enables a manipulation of the spontaneous emission of fluorescent materials embedded in the cavity by changing the optical mode density surrounding them [11]. A considerable body of literature has been published concerning the changes in profile, intensity and lifetime of the photoluminescence (PL) spectra of Er^{3+} ions and other materials embedded in F–P microcavities, which are interesting from a fundamental viewpoint, as well as for industrial applications [3–19]. Oxide-based dielectric materials are particularly suitable for fabricating PBG structures because they have wide transparency from the ultraviolet to the near-infrared, which is an important advantage compared with semiconductor materials which are usually used to prepare PBG structures for operation in the infrared. Furthermore, oxide-based dielectric materials have good resistance to temperature, corrosion and radiation as well [12]. Various techniques have been reported for the fabrication of F–P microcavities based on oxide dielectric materials, such

³ Author to whom any correspondence should be addressed.

as sputtering [12], ion plating [13] and sol–gel processing [3–9, 14–16]. The sol–gel method, based on wet chemistry, has two main advantages for the fabrication of PBG structures: it is a cheap and versatile technique to deposit alternating layers of different materials with controlled refractive index and thickness; it is a simple and highly flexible method to dope the dielectric films with various active materials. However, cracking easily takes place during sol–gel processing when the total thickness of the multilayer structure exceeds a value of around 1 μm , which is a serious shortcoming of this technique [15, 20]. This difficulty generally prevents the fabrication of PBG devices needing very complex structures or long working wavelengths by sol–gel processing.

In this paper, several high quality Er-doped F–P microcavities consisting of alternating silicate glass and titania films were prepared by a novel sol–gel technique. The thickest sample that was deposited without any cracking consisted of 124 dielectric layers and its thickness reached about 12 μm . All the prepared samples exhibited good optical quality. Their transmission spectra and the 1.5 μm PL of the dopant Er^{3+} ions were measured. The highest quality factor (Q) from these samples was 250. The Q factor is given by $Q = \lambda/\Delta\lambda$, where λ is the resonance wavelength of the microcavity and $\Delta\lambda$ is the resonance full width at half maximum (FWHM). A PL enhancement of up to 96 times at 1.5 μm was also observed. These results indicate that the presently reported sol–gel technique is well suited for application in the research and fabrication of low cost PBG devices. The preparation process and characterization of the prepared materials and structures are explained in detail.

2. Experiments

2.1. Sol–gel processing

A 1D F–P microcavity is composed of alternating high and low refractive index dielectric layers with an optical thickness of $\lambda/4$. The index contrast between the two materials should be as large as possible in order to obtain high reflectivity and a broad stop band with fewer dielectric periods [3–9, 16]. Titania and silicate glass films are two such materials. Their refractive indices in the optical region are approximately 2.2 and 1.45, respectively [3]; they have wide optical transparency and good chemical stability and they can be easily deposited by sol–gel [3–9, 14–16]. For resonance in tune with the peak position of the Er^{3+} PL at 1535 nm, the quarter-wave thickness of the silicate and titania films should be approximately 265 nm and 174 nm, respectively, given their refractive index values.

The sol–gel process started with the sol preparation. In this work, three sols were needed. A sol for silicate films, a sol for erbium-doped silicate films and a sol for titania films. The silicate sol was prepared by mixing 3 ml of tetraethylorthosilicate (TEOS), 6 ml of isopropanol and 0.48 ml of 0.01N HCl, with continuous stirring at 70 °C for 3 h. This was then diluted with 9 ml of isopropanol and 0.5 g of $\text{Al}(\text{NO}_3)_3$, leading to a silicate composition with 91 SiO_2 –9 $\text{AlO}_{1.5}$ (in mol%). In addition, for the case of erbium-doped and ytterbium co-doped silicate films, 0.06 g $\text{Er}(\text{NO}_3)_3$

and 0.12 g $\text{Yb}(\text{NO}_3)_3$ were also dissolved in the silicate sol, corresponding to the dopant concentrations of 1 mol% Er^{3+} and 2 mol% Yb^{3+} (on a cation basis). The co-dopant ytterbium is normally added to our standard composition in order to sensitize the Er^{3+} PL when pumped by 980 nm light by the energy transfer mechanism [6–9], although in the present case this effect has not been studied. The titania sol was prepared by mixing 2.5 ml of titanium isopropoxide with 3 ml of glacial acetic acid, followed by stirring for 1 h and dilution in 16 ml of absolute ethanol. All sols were aged for 24 h before film deposition. The PBG samples were fabricated by a multilayer deposition process. Alternating layers of silicate and titania films were deposited on the silicon substrates by spin-coating at 2000 rpm. Each layer was individually annealed in a muffle furnace at 1050 °C for 30 s, in order to relieve the stress in each cycle and prevent cracking. The thickness of each silicate layer was \sim 140 nm and that of each titania layer was \sim 60 nm. According to the previous estimation, approximately two silicate layers and three titania layers were needed to complete a low/high refractive index dielectric period. The thickness of the individual silicate and titania films could be finely adjusted by the volume of the solvent added to the precursor sols. F–P microcavities with two BMs consisting of 5, 7, 10 and 12 distributed Bragg reflector (DBR) periods each were prepared. From now on, such samples will be designated as 5-period, 7-period and so on. The silicate cavity films at the centre of the microcavity structures were deposited from an erbium-doped silicate sol, whereas all the other films were deposited from undoped sols. For each microcavity sample, a corresponding reference sample consisting only of the erbium-doped films was prepared from the same sols and by the same processing method, in order to determine the effects originating specifically from the microcavity structure. At the end of the deposition cycle, all samples were annealed at 1000 °C for one additional hour to reduce the residual OH group content, since the 1.5 μm Er^{3+} PL is highly sensitive to quenching by OH groups [21].

2.2. Characterization

The cross section of a multilayer structure consisting of two BMs with 10 periods each was observed using a FEG-SEM JEOL JSM-7001F in the back-scattered electron mode. The crystal phase of the titania films in the samples was determined by grazing incidence x-ray diffraction (GI-XRD) using a Bruker AXS D5000 x-ray diffractometer. The refractive indices of the silicate and titania films were determined by ellipsometry (HORIBA Jobin-Yvon model UVISEL NIR spectroscopic ellipsometer) and M-line spectroscopy (Metricon, 2010/M prism coupler) techniques. The transmission spectra of all the samples were measured with a Nicolet 5700 FTIR spectrometer (Thermo Electron Corporation). The 1.5 μm PL from the Er^{3+} ions was measured with a previously described standard setup [12]. The 514.5 nm line of a Coherent model Innova Sabre Ar^+ ion laser was used as the excitation source. The luminescence was dispersed by a 320 mm single-grating monochromator with a resolution of 2 nm and it was detected using a Hamamatsu photomultiplier

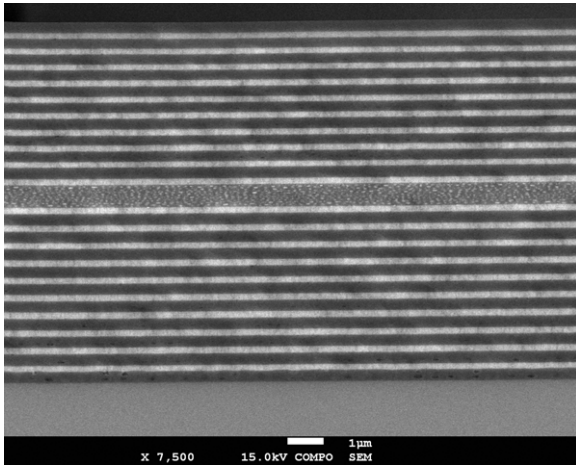


Figure 1. FEG-SEM cross section micrograph of a microcavity with two 10-period BMs deposited on a silicon substrate, in the back-scattered electron mode. The bright strips are titania layers and the dark strips are silicate glass. The estimated thickness of each silicate layer is 304 nm and that of each titania layer is 165 nm. The total thickness of the whole structure is 9988 nm.

tube and a standard lock-in technique. Since the cavity resonance is strongly dependent on the detection angle, all the PL spectra in this paper were measured with detection perpendicular to the multilayer structure.

3. Results and discussion

3.1. Sample preparation

In this work, all samples had good optical quality and were free of cracks. The thickest sample deposited had 24 low/high index periods, corresponding to a total of 124 individual layers of silicate and titania films. Figure 1 shows a SEM micrograph of the cross section of a sample with two 10-period BMs, i.e. a 10-period microcavity in the present nomenclature. The bright strips are titania layers and the dark ones are silicate glass layers. These dielectric films exhibit very good parallelism, their thickness is constant for each type of material and there is no visible mixing between them. For the sample of figure 1, the thickness of each silicate layer was estimated from the micrograph to be ~ 304 nm and that of each titania layer was ~ 165 nm. The total thickness of the whole structure was 9988 nm. So the thickness of a 12-period sample can be estimated to be $\sim 12 \mu\text{m}$. The micrograph shows the very good deposition quality of the present sol-gel technique.

It is believed that dividing each dielectric film into several thinner layers and annealing each layer at an appropriate high temperature are the key steps, which allow the present technique to prevent the cracking problem [15, 20]. Generally, cracking happens when the stress accumulated inside the film exceeds its mechanical strength [22]. During the sol-gel coating process, the sol adhering onto the substrate transforms into a gel film rapidly by evaporation of the solvent and the gel film is then densified to a glassy film by heat treatment at a sufficiently high temperature. Since the substrate allows only 1D shrinkage, stresses readily develop inside the densifying gel film. But the thinner the film, the lower the level of stress

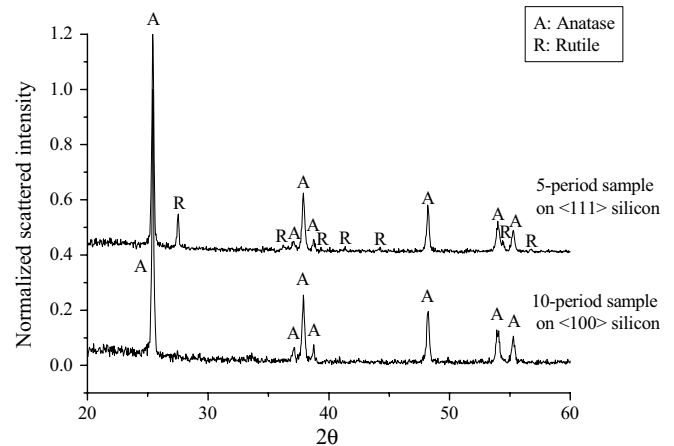


Figure 2. GI-XRD patterns of 5-period and 10-period F-P microcavities. The peaks corresponding to anatase (A) and rutile (R) are denoted. The 5-period sample was deposited on a $\langle 111 \rangle$ silicon wafer and the 10-period sample on $\langle 100 \rangle$ silicon. The titania films exhibit only the anatase phase on $\langle 100 \rangle$ silicon, whereas some rutile phase appears for films on $\langle 111 \rangle$ silicon substrate.

generated; therefore, for single layer deposition, cracking will not happen if the film is thin enough [22]. Annealing of the sample is performed after each individual deposition cycle in order to prevent the accumulation of residual stresses [20]. The silicate sol-gel film starts to change from the porous amorphous film to a glassy material when it is annealed at about 900°C [23]. When its original porous structure collapses and the film starts to densify, the stresses inside the film can be eliminated by this conversion process at an appropriate temperature. The annealing temperature must be high enough to densify the silicate film and to thoroughly eliminate the stress. However, too high a temperature will damage the deposited film and the substrate, evaporating the dopant species and introducing thermal stresses due to the thermal expansion mismatch between the substrate and the deposited films. In the present case, 1050°C was the experimentally determined appropriate temperature. Besides the coating technique, the aluminium present in the silicate film also helps. The addition of alumina has two purposes. One is that aluminium is known to increase the solubility of rare-earth ions in the silicate host, compared with pure silica [24–26]. The other is that the Al^{3+} ions can reduce the rigidity of the pure silica glass matrix, which also prevents stress accumulation.

3.2. Crystallization of titania films

The annealing step at high temperatures inevitably leads to titania film crystallization. The GI-XRD curves of a sample with two 5-period BMs and a sample with two 10-period BMs, respectively, are shown in figure 2. The 5-period sample was deposited on a $\langle 111 \rangle$ silicon wafer and the 10-period sample on $\langle 100 \rangle$ silicon. It was found that the TiO_2 crystal phase obtained depended upon the crystal orientation of the silicon substrate. When the $\langle 100 \rangle$ silicon wafer is used, the titania films exhibit only the anatase phase, whereas some rutile phase appears also for the films on the $\langle 111 \rangle$ silicon wafer. This phenomenon was observed on other samples as well. Because

Table 1. The values of the parameters in equation (1). There are three values for C , for pure silica glass, undoped sol-gel derived silicate glass and erbium-doped sol-gel derived silicate glass.

Parameters in equation (1)	Value
A_1	0.685 478
B_1 (μm^2)	0.004 597
A_2	0.418 637
B_2 (μm^2)	0.013 417
A_3	0.901 152
B_3 (μm^2)	98.299 634
C (pure silica glass)	0
C (undoped silicate film)	-0.0063
C (Er-doped silicate film)	-0.0020

the refractive indices of anatase and rutile are different, the unique phase on the $\langle 100 \rangle$ silicon substrate is preferred in view of the refractive index stability. A silica glass substrate was also tested, but a thick, good quality PBG structure could not be deposited, probably because of the poor thermal conductivity of silica glass.

The average TiO_2 crystal size in the prepared samples was estimated to be 65–95 nm based on XRD line broadening, using the Scherrer equation [27]. This result was similar to that of [15]. In theory, large crystal sizes will reduce the optical quality of the PBG structure due to light scattering, but the optical properties of the present samples proved to be good, nevertheless, as discussed later. One possible explanation is that the dimensions of several tens of nanometres are still much smaller than $1.5 \mu\text{m}$ (they are $\sim \lambda/20$) and the effective light propagation distance in the PBG structure is of the order of a few micrometres only. These two reasons make the scattering effect not very serious. Of course, avoiding crystallization would always be good, which could be achieved by shortening the total annealing time during preparation [15], especially when the active dopant materials are less sensitive to OH groups than Er^{3+} ions. On the other hand, the present result demonstrates that crystallization in PBG devices is not such a serious problem as in waveguides.

3.3. Refractive index

The refractive index of the deposited silicate glass and titania films was studied in detail by M-line spectroscopy and spectroscopy ellipsometry (SE). It was found that the refractive index of the sol-gel derived silicate glass can be simulated by moving the dispersion curve of pure silica glass vertically by a constant. In mathematical terms, the refractive index can be expressed by

$$n_{\text{silicate}} = \sqrt{1 + \frac{A_1 \lambda^2}{\lambda^2 - B_1} + \frac{A_2 \lambda^2}{\lambda^2 - B_2} + \frac{A_3 \lambda^2}{\lambda^2 - B_3}} + C. \quad (1)$$

The values of the parameters A_1 , B_1 , A_2 , B_2 , A_3 , B_3 and C are listed in table 1. For pure silica glass ($C = 0$), equation (1) is a three-term Sellmeier equation and the difference between the calculated results and the values from [28] is less than 1.5×10^{-5} in a wide wavelength range from 210 to 2450 nm. For the sol-gel derived silicate glass, a parameter C best

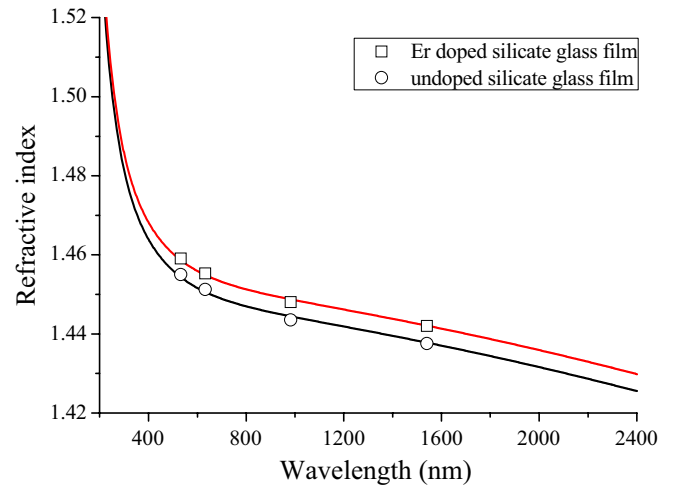


Figure 3. Dispersion curves of the erbium-doped and undoped sol-gel derived silicate glass films. The symbols refer to results measured by the prism coupler. The two solid lines are the results of the fitting by equation (1). The refractive index of erbium-doped sol-gel silicate glass was higher by 0.004 than that of the undoped one.

fitted the calculated values to those measured by M-line spectroscopy. The fitted dispersion curves were also compared with the SE results, simultaneously. The final results are shown in figure 3 and the fitted values of C are listed in table 1. The two solid lines in figure 3 are the simulated dispersion curves and the symbols are values measured by M-line spectroscopy, using the prism coupler at four different wavelengths: 532, 632.8, 983 and 1540 nm. The measured data and the simulated curve agree very well. In figure 3, the top line refers to the erbium-doped film and the bottom line to the undoped one. The refractive index of the erbium-doped film was larger by ~ 0.004 than that of the undoped film, due to the presence of the heavy rare-earth ions. This small difference can be compensated by adding more alumina to the undoped sol, if necessary. In the present case, however, the $\sim 0.3\%$ difference does not make an observable effect.

The refractive index of the titania films was too large to be measured by our prism coupler. Therefore, a model taken from [29] was used to analyse their ellipsometric curves. The model is described by the following equations:

$$\begin{aligned} n_{\alpha}(E) &= n_{\alpha}(\infty) + \frac{B_{\alpha}E + C_{\alpha}}{E^2 - BE + C}, \\ k_{\alpha}(E) &= \frac{A(E - E_g)^2}{E^2 - BE + C}, \\ B_{\alpha} &= \frac{A}{Q} \left(-\frac{B^2}{2} + E_g B - E_g^2 + C \right), \\ C_{\alpha} &= \frac{A}{Q} \left((E_g^2 + C) \frac{B}{2} - 2E_g C \right), \\ Q &= \frac{1}{2} \sqrt{4C - B^2}. \end{aligned} \quad (2)$$

The fitted parameters are listed in table 2. The calculated refractive index is shown in figure 4 by a dashed line. In

Table 2. Values of the fitting parameters in equation (2).

Parameters in equation (2)	Value
A	0.0382
B (eV)	8.1454
C (eV ²)	16.6685
n_{∞}	2.0385
E_g (eV)	2.0934

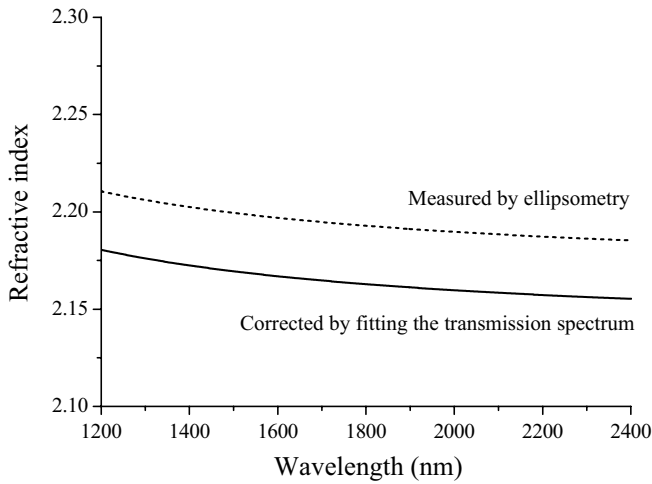


Figure 4. Dispersion curves of the titania films. The dashed line is the result of the spectroscopic ellipsometry measurement. The solid line is the curve corrected by fitting the transmission spectrum of figure 5.

the range from 1200 to 2400 nm, in which the transmission spectra were measured, the dispersion curve of the sol-gel derived titania film slowly decreases around a value near 2.2, which is typical of TiO₂ material.

3.4. Transmission spectra

The transmission spectra of the 1D PBG structures can be calculated by the transfer matrix method (TMM) using the refractive index and the thickness of each layer [7]. The simulated and measured transmission spectra of the 10-period sample of figure 1 are shown in figure 5. The initial thickness estimate for the dielectric layers in the simulation was derived from figure 1 and the refractive index values have been discussed above. Since the silicon substrate used was a one side polished wafer, the measured spectrum cannot be directly compared with the theoretical curve due to light scattering by the unpolished surface. So the two spectra in figure 5 were both normalized to their maximum values. In figure 5, the dashed line is the curve simulated by the TMM and the solid line is the measured transmission spectrum using FTIR. It is shown that the theoretical curve agrees very well with the measured spectrum in the whole range from 1200 to 2400 nm, including the position and width of the stop band, the defect peak position and almost all the fringes. This means that the models developed in section 3.3 for the refractive index work well and can be used in future calculations. When obtaining the simulated curve of figure 5, the thickness of the silicate glass and titania films and the refractive index

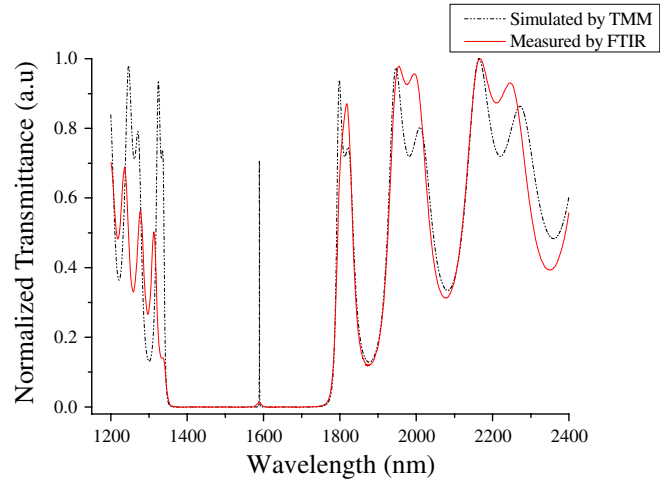


Figure 5. Transmission spectra of the microcavity sample shown in figure 1. The solid curve was measured by FTIR. The dashed line is the curve fitted by the TMM.

of the titania material were slightly adjusted for best fitting. The fitted thicknesses were 323 nm for the silicate glass film and 138 nm for titania, respectively. Since the resolution of figure 1 is 12.5 nm for one pixel, the thickness adjustment was actually ~ 2 pixels. The best fitted refractive index of the titania film was smaller by 0.03 than the values estimated from ellipsometry. The correction was also close to the precision of the ellipsometer. The corrected dispersion curve is drawn in figure 4 by a solid line.

An obvious difference between the simulated and measured transmission spectra of figure 5 is that the simulated defect peak inside the stop band was intense and sharp, whereas the measured one was quite small. This difference can be attributed to two facts. One is the limited spectral resolution of the FTIR equipment; the other is a small fluctuation in the resonance wavelength depending on the sample area actually probed, which may be caused by slight point-to-point variations in film thickness. Both factors translate into convoluting the defect peak with a window function. When the FWHM of the peak is smaller than the window width, the resulting peak will be broadened and dwarfed. For a given effective window width, the sharper the original peak, the lower will be the measured intensity. The Q factor ($\lambda/\Delta\lambda$) of a F-P microcavity increases with the reflectivity of its BMs, which increases with the number of its DBR periods. So a high-period microcavity will have a sharper defect peak (smaller $\Delta\lambda$), which will also contribute to a corresponding lower intensity if $\Delta\lambda$ is smaller than the effective window width. This is the case illustrated in figure 6, in which four transmission spectra, for the samples with different numbers of BM periods on each side, are drawn together. The number of periods of each BM is written next to the sample spectrum and all the curves have been moved vertically for better viewing. It is obvious that the samples with more BM periods have sharper and lower intensity defect peaks.

The resonance wavelength of the F-P microcavity is very sensitive to the thickness of its dielectric layers. According to the refractive indices obtained in figures 3 and 4, a thickness

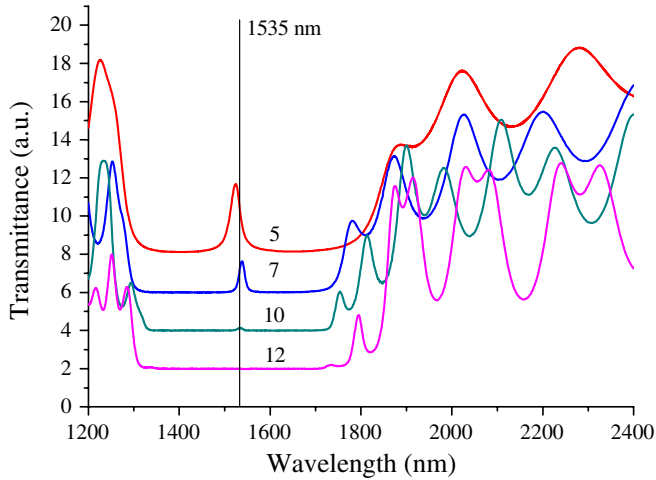


Figure 6. Transmission spectra of microcavity samples with 5, 7, 10 and 12 BM periods on each side. The number of periods is indicated next to each curve and all the curves were moved vertically for better viewing.

of 267 nm for the silicate glass film and 177 nm for the titania films will set the resonance wavelength of the F–P microcavity exactly at 1535 nm. If these two thicknesses deviate by a small value (e.g. ± 100 nm), the TMM simulation shows that the actual deviation in the resonance wavelength can be estimated by

$$\Delta\lambda = 3.386\Delta d_{\text{Si}} + 3.469\Delta d_{\text{Ti}}, \quad (3)$$

where $\Delta\lambda$ and Δd are the deviations of the resonance wavelength relative to 1535 nm and the thickness of the dielectric layers, respectively. For instance, the simulated layer thicknesses for the sample of figure 1 were 323 nm for silicate glass and 138 nm for titania, so its resonance wavelength calculated using equation (3) is 1589 nm, which is equal to the value measured in figure 5. Equation (3) means that a 1 nm deviation in the dielectric layer thickness will introduce an error of more than 3 nm in the resonance wavelength position. This very precise thickness control needed is one of the main difficulties during sample preparation. The thickness of the deposited film can be finely adjusted by changing the volume of the solvent added to the precursor sols. The resonance wavelengths of the samples in figure 6 were all designed to be equal to ~ 1535 nm through very careful sol–gel processing in each step. The variations in dielectric layer thickness of microcavities with a large number of DBR periods can be estimated by equation (3). According to the above discussion, the broadening of the defect peak in the transmission spectra comes from the spectral resolution limit of the FTIR equipment and the fluctuations in dielectric layer thickness. For example, the FWHM of the defect peak for the 10-period sample of figure 6 is 13.6 nm. Even if one were to assume that all this spectral broadening was due to the non-uniformity of the sample, the actual average point-to-point variation in film thickness calculated by equation (3) would be only $\Delta d \sim 4$ nm. These results demonstrate the possibility of using the present sol–gel technique for the fabrication of precise PBG devices. Note that all the samples in this work

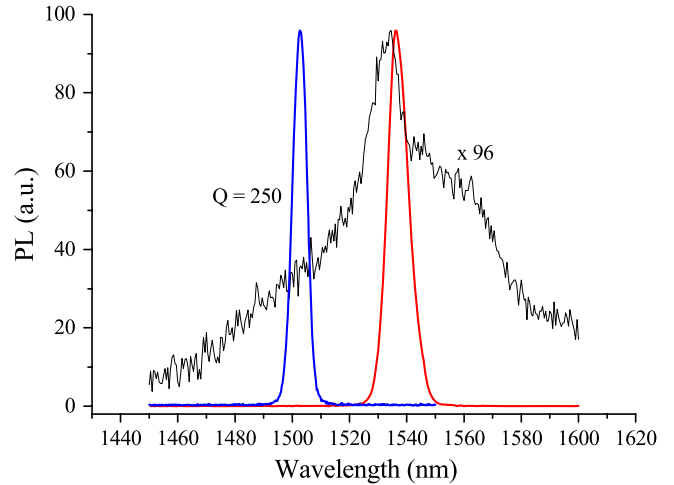


Figure 7. PL spectra of two different microcavity samples with 10-period BMs on each side and a reference sample. The broad spectrum is from the reference sample. The two spectra from microcavities are drawn as thick solid lines. The microcavity corresponding to the PL spectrum on the right (1536 nm) was deposited using the same erbium-doped sol as the reference sample. The reference spectrum was magnified 96 times to have the same normalized intensity. The intensity of the PL spectrum on the left (1503 nm) was normalized to that of the right one. The Q factor estimated from this spectrum is 250.

were prepared manually in a common laboratory. Higher uniformity and precision should be achievable by improving the deposition setup, including a clean room environment and possible automation.

3.5. Photoluminescence

The quality of a F–P microcavity is normally judged by its Q factor. The PL enhancement factor is also determined when luminescent materials are present inside the cavity [12–17]. The 1.5 μm PL of all the erbium-doped samples in this work was measured. The PL enhancement factor can be estimated by comparing the PL intensity from a microcavity with that of its reference sample. This PL enhancement originates from the increase in the emission rate of the erbium ions coupled to the resonance optical mode of the microcavity and the profile of the PL is similar to the resonance peak in the transmission spectrum [11, 16, 19]. For this reason, the Q factor can also be estimated from the PL spectrum by calculating $\lambda/\Delta\lambda$ at the resonance wavelength [12, 14].

The two best results among all the samples measured are shown in figure 7 together with a typical Er^{3+} PL spectrum in silicate glass from a reference sample. The spectrum of the reference sample, shown by a thin solid line, was broad, whereas the two spectra from the microcavities, drawn in thick solid lines, have a symmetric and much sharper profile. The PL intensity of the microcavity samples was enhanced compared with the reference. The sharp peak at 1536 nm was given by a 10-period microcavity that was deposited using the same erbium-doped sol as the reference sample in figure 7. But the reference spectrum had to be amplified 96 times to have the same peak intensity as the microcavity spectrum. The value of 96 was the best enhancement factor obtained in this

work. The sharp peak at 1503 nm in figure 7 was from another 10-period microcavity, whose PL intensity was normalized to that of the peak on the right-hand side. The highest Q factor of 250 was estimated from this spectrum. The above Q factor and enhancement are typically good values for a F–P microcavity made from oxide-based dielectric materials [12, 14–16]. This again demonstrates that the present sol–gel processing technique appears suitable for the fabrication of high quality 1D PBG devices.

4. Conclusions

Devices based on 1D PBG structures are of interest in fundamental research and for industrial applications as well. The sol–gel technique may provide a cheap and easy way to fabricate such devices. An optimized sol–gel process is reported in this paper to produce 1D PBG structures of good optical quality. Several erbium-doped F–P microcavities were prepared and characterized. The thickest sample contained two BMs having 12 DBR periods each. Its total thickness reached $\sim 12\ \mu\text{m}$. A best Q factor of 250 and the highest PL enhancement of 96 times were obtained for 10-period microcavities. The details of the present technique, including the sol–gel process, the crystallization of titania films and the refractive index of all the deposited materials, were all discussed in detail. The transmission spectra simulated using the obtained material parameters agreed well with the actually measured curves. These results demonstrate that the present sol–gel process is a potential technique to be applied for the fabrication of 1D PBG devices.

Acknowledgments

The authors wish to thank Professor Olinda Conde, from Faculdade de Ciências da Universidade de Lisboa, for her help with the XRD measurements. One of the authors (YL) would also like to thank FCT (Fundação para a Ciência e a Tecnologia) for support under an Assistant Researcher contract at Instituto Superior Técnico. Two of the authors (AC and MF) also wish to acknowledge support from PAT-FaStFal and COST MP0702 research projects.

References

- [1] Yablonovitch E 1987 *Phys. Rev. Lett.* **58** 2059
- [2] John S 1987 *Phys. Rev. Lett.* **58** 2486
- [3] Almeida R M and Rodrigues A S 2003 *J. Non-Cryst. Solids* **326–327** 405
- [4] Almeida R M and Portal S 2003 *Curr. Opin. Solid State Mater. Sci.* **7** 151
- [5] Almeida R M, Gonçalves M C and Portal S 2004 *J. Non-Cryst. Solids* **345–346** 562
- [6] Almeida R M, Marques A C and Portal S 2005 *Opt. Mater.* **27** 1718
- [7] Almeida R M and Marques A C 2006 *J. Non-Cryst. Solids* **352** 475
- [8] Almeida R M, Marques A C, Chiasera A, Chiappini A and Ferrari M 2007 *J. Non-Cryst. Solids* **353** 490
- [9] Almeida R M and Marques A C 2009 *J. Mater. Sci.: Mater. Electron.* **20** S307
- [10] Ünlü M S and Strite S 1995 *J. Appl. Phys.* **78** 607
- [11] Vredenberg A M, Hunt N E J, Schubert E F, Jacobson D C, Poate J M and Zydzik G J 1993 *Phys. Rev. Lett.* **71** 517
- [12] Chiasera A, Belli R, Bhaktha S N B, Chiappini A, Ferrari M, Jestin Y, Moser E, Righini G C and Tosello C 2006 *Appl. Phys. Lett.* **89** 171910
- [13] Rigneault H, Amra C, Robert S, Begon C, Lamarque F, Jacquier B, Moretti P, Jurdyc A M and Belarouci A 1999 *Opt. Mater.* **11** 167
- [14] Bellessa J, Rabaste S, Plenet J C, Dumas J, Mugnier J and Marty O 2001 *Appl. Phys. Lett.* **79** 2142
- [15] Rabaste S, Bellessa J, Brioude A, Bovier C, Plenet J C, Brenier R, Marty O, Mugnier J and Dumas J 2002 *Thin Solid Films* **416** 242
- [16] Jasieniak J, Sada C, Chiasera A, Ferrari M, Martucci A and Mulvaney P 2008 *Adv. Funct. Mater.* **18** 3772
- [17] Schubert E F, Vredenberg A M, Hunt N E J, Wong Y H, Becker P C, Poate J M, Jacobson D C, Feldman L C and Zydzik G J 1992 *Appl. Phys. Lett.* **61** 1381
- [18] Schubert E F, Hunt N E J, Micovic M, Malik R J, Sivco D L, Cho A Y and Zydzik G J 1994 *Science* **265** 943
- [19] Golubev V G, Dukin A A, Medvedev A V, Pevtsov A B, Sel'kin A V and Feoktistov N A 2001 *Semiconductors* **35** 1213
- [20] Syms R R A, Holmes A S, Huang W, Schneider V M and Green M 1998 *J. Sol–Gel Sci. Technol.* **13** 509
- [21] Ferrari M 2005 *Handbook of Sol Gel Science and Technology: Processing, Characterization and Applications* vol 2 ed S Sakka (Boston, MA: Kluwer) p 359
- [22] Brinker C J and Scherer G W 1990 *Sol–Gel Science: The Physics and Chemistry of Sol–Gel Processing* (San Diego, CA: Academic) p 506
- [23] Li Y, Liu L, He Z, Tang H, Xiao S, Xu L and Wang W 2004 *J. Sol–Gel Sci. Technol.* **30** 29
- [24] Almeida R M, Du X, Barbier D and Orignac X 1999 *J. Sol–Gel. Sci. Technol.* **14** 209
- [25] d'Acapito F, Mobilio S, Gastaldo P, Barbier D, Santos L F, Martins O and Almeida R M 2001 *J. Non-Cryst. Solids* **293–295** 118
- [26] Alombert-Goget G, Gaumer N, Obriot J, Rammal A, Chaussedent S, Monteil A, Portales H, Chiasera A and Ferrari M 2005 *J. Non-Cryst. Solids* **351** 1754
- [27] Patterson A L 1939 *Phys. Rev.* **56** 978
- [28] Philipp H R 1998 *Handbook of Optical Constants of Solids* vol 1 ed E D Palik (San Diego, CA: Academic) p 749
- [29] Forouhi A R and Bloomer I 1998 *Handbook of Optical Constants of Solids* vol 2 ed E D Palik (San Diego, CA: Academic) p 161